Catalysis Letters 54 (1998) 227–233

Characterisation of acid-treated bentonite. Reactivity, FTIR study and ^{27}Al MAS NMR

D. Haffad *, A. Chambellan and J.C. Lavalley

UMR 6506: Catalyse et Spectrochimie, ISMRAa – Université, 14050 Caen, France
E-mail: spectrocat@ismra.unicaen.fr

Received 14 April 1998; accepted 10 July 1998

Acid-treated bentonite shows a catalytic activity towards decomposition of isopropanol due to overall acidity whereas the selectivity accounts for the nature of its acid sites. The examination of the IR spectra using different basic probes such as 2,6-dimethylpyridine, pyridine and CD_3CN shows the presence of various types of acid sites. The Lewis acid sites, considered to be the most abundant, are well characterised by pyridine and CD_3CN adsorption. In contrast, lutidine adsorption reveals both the existence of Brønsted acid sites and the presence of hydroxyl groups characteristic of beidellite. The potential site created by Al in tetrahedral layers is confirmed by using ^{27}Al MAS NMR.

Keywords: bentonite, acidity, FTIR, test reaction

1. Introduction

One of the techniques used leading to a high surface area and porosity of bentonite (montmorillonite) is acid activation. Inevitably as Al^{3+} and other metal ions are leached, the cation exchange capacity and overall acidity of clays drop [1–3]. This work aims to characterising the residual acidity of an acid-treated bentonite.

Bentonite and acid-treated montmorillonite have been used as acidic heterogeneous catalysts [1,4] and catalyst supports [1]. Recently, the preparation of ethyl ether by dehydration of ethanol has been reported using an acid-treated bentonite [5].

Moreover, using a quick test for acidity evaluation [6,7], it has been found that a commercial acid-treated bentonite exhibits high activity in isopropanol decomposition in moderate conditions producing isopropyl ether and/or propene.

It is, therefore, interesting to determine the nature of acid sites of the acid-treated bentonite by adsorption of basic probes using infrared spectroscopy and solid-state ^{27}Al MAS NMR as the non-destructive characterisation of Al sites in clays [8,9].

2. Experimental

The experiments were carried out on a "commercially" acid-treated bentonite (industrially prepared in Algeria under the name of acid-activated bentonite). The starting material is a natural bentonite treated industrially by using an acid attack (H_2SO_4) at 100 °C for 12 h. The activation process is followed by washing, filtration, drying, crushing and conditioning.

Chemical composition: silica, alumina and other elements were analysed by X-ray fluorescence. BET surface was measured by nitrogen adsorption (77 K) using a Micromeritics ASAP 2000 sorptiometer. XRD was performed on powder using Cu K_α radiation (automatic diffractometer APD 1700). The ^{27}Al MAS NMR spectra were recorded on a Bruker spectrometer at 104 MHz frequency.

The acidity evaluation was performed on the base of propan-2-ol transformation under helium atmosphere in a quartz microflow reactor at atmospheric pressure. The sample (160 mg) was activated at 623 K under helium flow (20 ml/min) for 2 h, then cooled down to 333 K. A propan-2-ol flow ($P_e = 1.2$ Torr) diluted in helium was then introduced. The reaction was studied in the temperature range 333–393 K. The products formed were analysed on-line by gas chromatography equipped with a FID detector.

The acidity of commercial acid-treated bentonite was probed by pyridine, 2,6-dimethylpyridine and CD_3CN. Samples (15 mg) were pressed into disks placed in the IR cell, then activated *in situ* by heating under vacuum at 723 K for 2 h. After cooling to room temperature, they were evacuated by increasing temperature. The spectra were recorded with a Nicolet 60 SX FTIR spectrometer with accumulation of 256 scans at 4 cm^{-1} resolution.

3. Results

The cation exchange capacity (CEC) was determined by using adsorption of methylene blue [10] and calcium exchange methods [11]; the elemental analysis and the BET surface area of the commercial sample are given in table 1.

The XRD pattern of the acid-treated bentonite shows a basal spacing of 15.04 Å. The peak positions observed in

* To whom correspondence should be addressed.

the range 2θ 3–40° are characteristic of montmorillonite and beidellite in comparison with the values reported for ideal montmorillonite and beidellite in the literature. This means that the sample used presents a character of beidellite markedly near that of montmorillonite, which latter is preserved despite the acid treatment.

The catalytic activity of the bentonite sample towards propan-2-ol decomposition is shown (figure 1) in different stationary conditions.

The propan-2-ol conversion occurs at 333 K, leading to both propene and isopropyl ether. When the temperature reaches 353 K, only propene is formed, the maximum activity is observed at 393 K.

The infrared study has been undertaken to provide some information for the interpretation of the residual acidity of acid-treated bentonite.

Figure 2(a) shows the spectrum of the acid-treated bentonite activated by heating under vacuum at 723 K; it

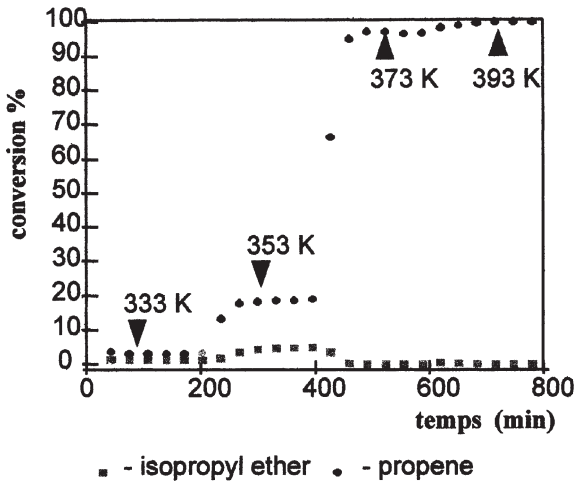

Figure 1. Propan-2-ol transformation under helium on acid-treated bentonite activated at 623 K: T_R = 333–393 K, Q_v = 20 ml/mn, W/F = 1.77 kg mol^{-1} h^{-1}.

Table 1
Chemical composition (%), cation exchange capacity and BET surface area of acid-treated bentonite.

SiO_2	Al_2O_3	Fe_2O_3	CaO	MgO	TiO_2	K_2O	Na_2O	Loss on ignition	CEC (meq/100 g)	BET (m^2/g)
69.39	14.14	1.16	0.30	1.07	0.16	0.79	0.5	11	56[a]/50[b]	169

[a] Calcium exchange method.
[b] Adsorption of methylene blue.

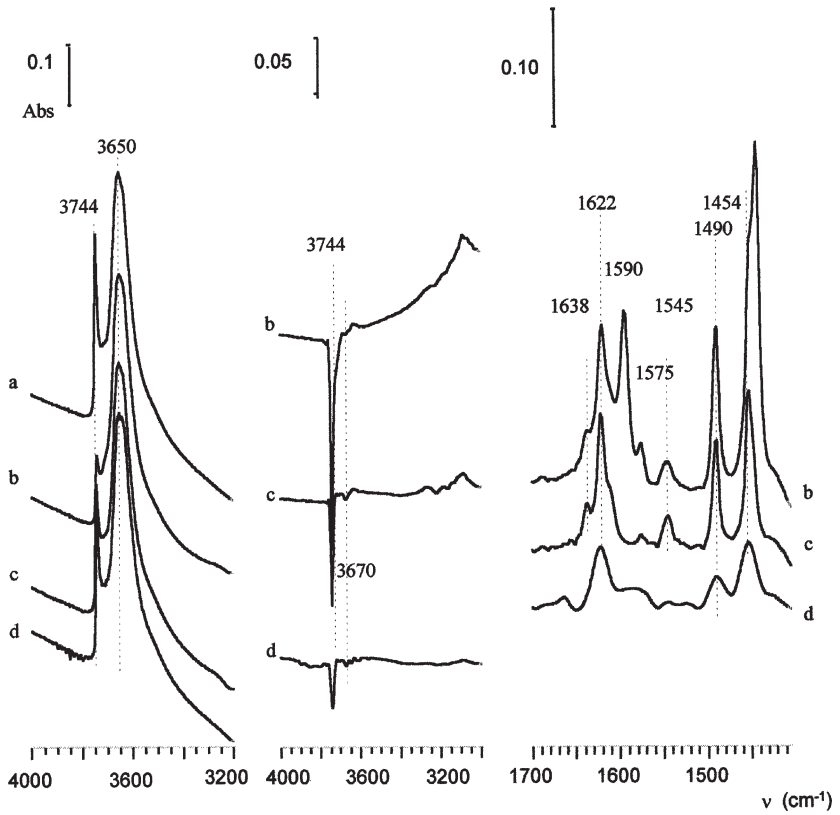

Figure 2. Adsorption of pyridine on acid-treated bentonite activated under vacuum at 723 K: (a) background, (b) evacuation at room temperature, (c) evacuation at 423 K and (d) evacuation at 573 K.

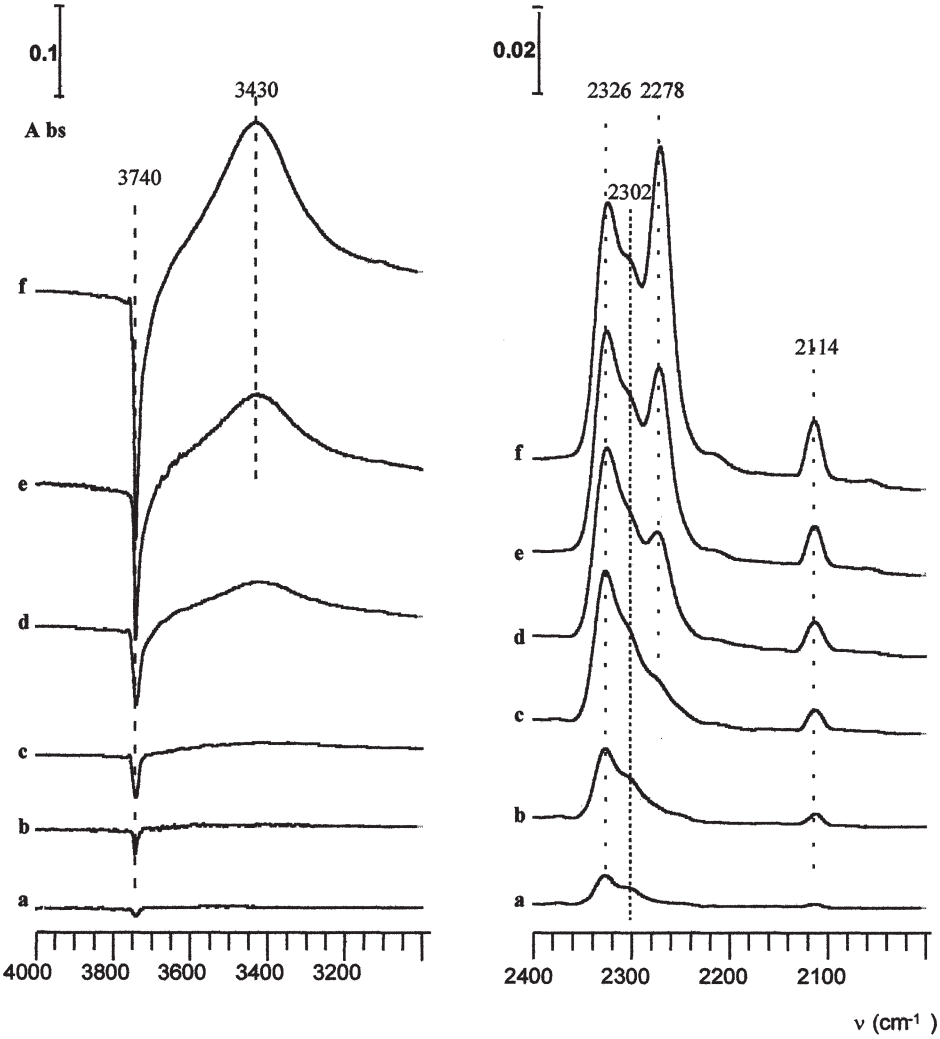

Figure 3. Adsorption of CD_3CN (μmol) at room temperature on acid-treated bentonite activated under vacuum at 723 K: (a) 0.16, (b) 0.32, (c) 0.64, (d) 1.28, (e) 2.56 and (f) 1 Torr at equilibrium.

presents two ν(OH) bands at 3744 and 3650 cm^{-1}. The first is assigned to silanol groups and the second, at lower frequency, may arise from hydroxyl groups bridging Al and Fe ions in octahedral positions [12] as the acid-treated bentonite contains a small proportion of Fe ions.

In order to evaluate the type of acidic sites presented by the sample, infrared spectroscopy (FTIR) of adsorbed bases has been applied.

(i) Pyridine ($pK_b = 8.8$) interacts with Lewis acid sites (LPy) giving rise to characteristic IR bands (figure 2) at 1620 cm^{-1} (ν_{8a}) and 1454 (ν_{19b}) [13]. The wavenumber of the ν_{8a} band provides information on the strength of LPy sites and the intensity of the (ν_{19b}) band is related to the number of LPy sites. Pyridine also interacts with Brønsted acid sites (BPy), resulting in the appearance of the band at 1545 cm^{-1} which is accompanied by a shoulder at 1638 cm^{-1} [11]. Note that the band at 1490 cm^{-1} contains a contribution of both Lewis and Brønsted acid sites [14,15]. In the ν(OH) region, the band at 3650 cm^{-1} remains inert in presence of pyridine, whereas the subtracted spectra (figure 2) show negative absorbances at 3744 (silanol) and 3670 cm^{-1}, but the decrease on adsorption is large at 3744 cm^{-1} showing that the involvement of SiOH groups is far-and-way dominant.

Following evacuation of pyridine at different temperatures, the band at 1545 and 1638 cm^{-1} resists until 423 K and disappears at 573 K, whereas the intensities of the other bands (1454, 1490, 1622 cm^{-1}) are unaffected by evacuation at 423 K but strongly decrease at 523 K. Note that the ν_{8a} wavenumber (1620–1622 cm^{-1}) is very high, showing the presence of strong LPy sites. In the ν(OH) region, the evolution with temperature is equivalent. However, some hydroxyl groups (3744 cm^{-1}) are still affected by pyridine and the band at 3670 cm^{-1} is scarcely detectable after evacuation at 573 K.

(ii) The CD_3CN probe can form surface nitrile species [16,17]. CD_3CN has been introduced by increasing doses on the studied sample. The spectrum obtained (figure 3) through the adsorption of small amounts shows the presence of three bands at 2326 [ν(CN)], 2114 [$\nu_s(CD_3)$], 2320 cm^{-1} and the appearance of a negative absorbance in the range of silanol groups at 3744 cm^{-1}.

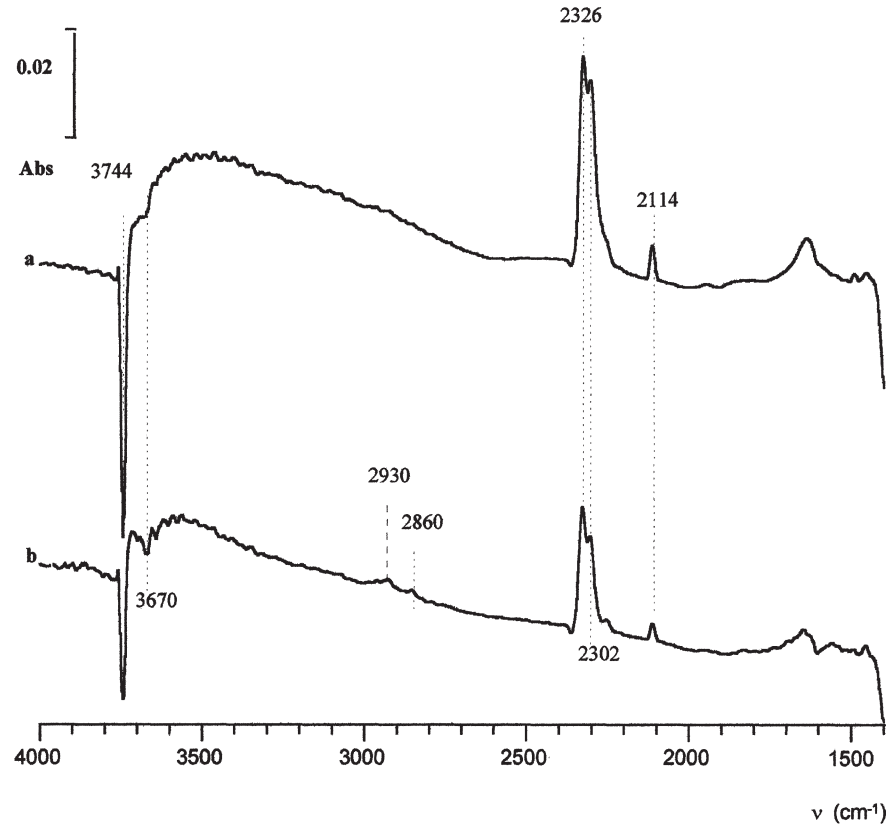

Figure 4. Adsorption of CD_3CN on acid-treated bentonite activated under vacuum at 723 K: (a) evacuation at room temperature and (b) evacuation at 423 K.

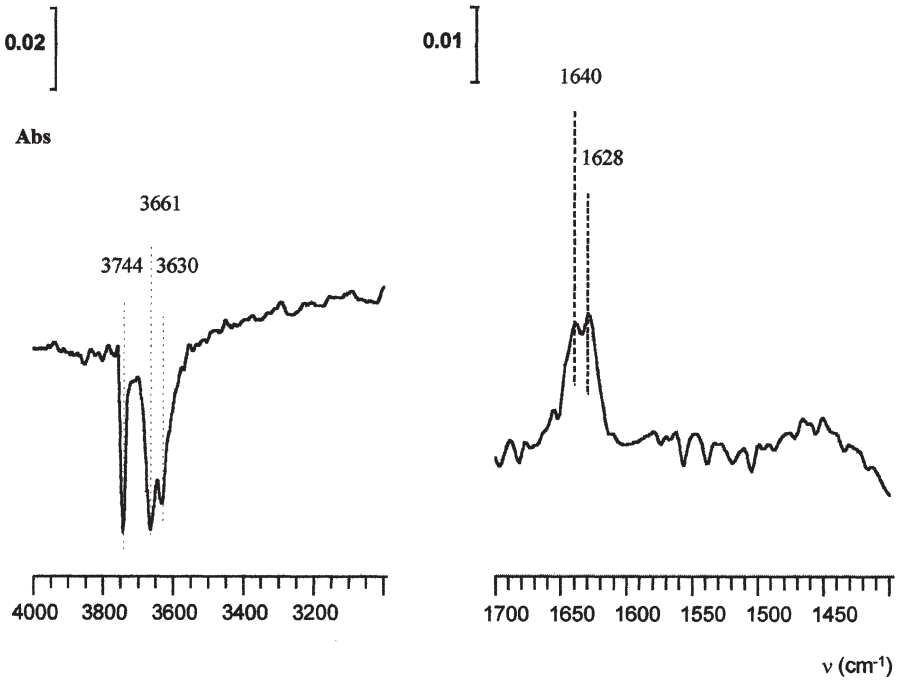

Figure 5. Adsorption of lutidine followed by evacuation at 423 K on acid-treated bentonite activated under vacuum at 723 K.

When a large amount of CD_3CN is introduced, the intensity of the bands at 2326 and 2114 cm^{-1} increases and reaches a maximum whereas the band (shoulder) at 2302 cm^{-1} remains almost unaffected. The wavenumber of the band at 2326 cm^{-1} reflects species associated with strong Lewis acid sites [16]. The band at 2302 cm^{-1} is probably due to CD_3CN interaction with Brønsted acid sites to form strongly hydrogen-bonded species.

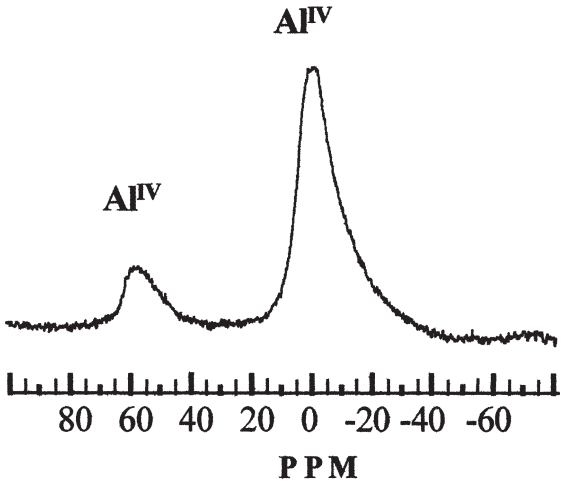

Figure 6. ^{27}Al MAS NMR spectra of acid-treated bentonite.

The presence of the band at 2278 cm^{-1} could be due to CD_3CN interaction with silanols [17]. This interaction is of the hydrogen bond type as shown by the appearance in the ν(OH) region of a rather broad band at 3430 cm^{-1}.

After evacuation at room temperature (figure 4), the bands at 2326, 2302 (weak) and 2114 cm^{-1} resist. Their intensity decreases by evacuation at 423 K and we note the presence of two bands at 2930 and 2860 [$\nu(CH_3)$] due to an exchange effect. In the ν(OH) region, as in the case of pyridine, the band (very weak) at 3670 cm^{-1} and some of silanol groups remain perturbed.

(iii) 2,6-dimethylpyridine (lutidine, $pK_b = 7.3$), which is a stronger base than pyridine [18], has been used for characterising Brønsted acid sites [13,19].

LuH^+ species (lutidinium) shows IR bands in the 1620–1650 cm^{-1} range (figure 5) characteristic of lutidine adsorption on Brønsted sites [18]. In the ν(OH) region, the negative absorbance at 3744 cm^{-1} is accompanied by other negative bands at 3661 and 3630 cm^{-1}.

After evacuation at room temperature or at 423 K, we note the presence of bands at 1643 and 1628 cm^{-1} due to lutidine adsorbed on Brønsted sites with the same hydroxyl groups remaining affected.

Figure 6 shows two signals, that at 57.28 ppm corresponding to tetrahedrally coordinated aluminium is close to that observed for Al^{IV} (58 ppm) in the case of zeolites [20] but is slightly lower than that of Texas montmorillonite (60 ppm) after acid treatment [9]. The second signal at 0.412 ppm (Al^{VI}) corresponds to aluminium in an octahedral position. They show the existence of two kinds of Al in tetrahedral (Al^{IV}) and octahedral (Al^{VI}) positions.

4. Discussion

The study of the residual acidity of acid-treated bentonite in the decomposition of propan-2-ol shows the formation of isopropyl ether and/or propene in moderate conditions. The selectivity of the reaction depends on the reaction temperature.

At low temperature (between 333 and 353 K), both isopropyl ether and propene are formed; the formation of isopropyl ether requires a Brønsted acidity. It is apparent, therefore, that the source of protons is derived from the catalyst itself via the hydration of the interlayer space and of the interlayer cations or part of hydroxyl groups (silanol). However, it is remarkable that at temperatures equal or higher than 373 K, only propene is formed. The absence of ether above 373 K and the inertia of pure silica (Degussa) for the same reaction seem to reveal that the weak acidity of silanol is no more operating. Conversely, the conversion into ether and propene, below 373 K and for which the desorption of the water formed does not seem easy, is in favour of the presence of hydrated interlayer cations.

The role of interlamellar water was evidenced in the ether production from hexan-2-ol, for which ether appears to cease when all the original interlamellar water has been consumed [21]. It is known that the interlayer cations such as Al^{3+} and Fe^{3+} present a high polarising power [22]. Some of these remaining cations after acid treatment (table 1) can produce a high interlayer acidity due to the high degree of dissociation of water adsorbed in the interlamellar space of layer lattice silicates of the smectite family [23,24]:

$$[M(OH_2)_m]^{Z+} \rightleftharpoons [M(OH_2)_{m-1}OH^-]^{Z+} + H^+$$

In our conditions (reaction controlled under helium flow), the absence of isopropyl ether above 100 °C suggests the desorption of water formed during the reaction and the formation of propene seems to involve surface acid sites, principally of Lewis acid type. This hypothesis has been confirmed by infrared study.

The qualitative analysis of residual acidity using pyridine [24–26] shows the formation of different species: adsorbed pyridine on Brønsted acid sites, species coordinated to Lewis acid sites and other species bonded via surface hydroxyl groups. However, their stability, followed by evacuation at different temperatures, appears quite different. Only the species coordinated to Lewis acid sites persist at 573 K and perturb the SiOH groups indirectly as in the case of amorphous silica–alumina [27]. In that case the residual acidity of acid bentonite is principally constituted by Lewis acid sites present on the surface [28].

As in the case of pyridine, CD_3CN reveals the presence of various types of acid sites. Indeed the adsorption of small amounts of this probe gives rise to $\nu(C{\equiv}N)$ bands at 2326 and 2302 cm^{-1}.

The first band well reflects species associated with strong Lewis acid sites [16] which are the most abundant. Howell [29] and Yurchenko [30] reported that all the Lewis acids containing a CUS aluminium atom gave rise to a band at 2328 cm^{-1}, shifted by 65 cm^{-1} with respect to the original $\nu(C{\equiv}N)$ vibrational mode in the liquid phase.

Considering the second band at 2302 cm^{-1}, it seems that CD_3CN less basic than pyridine interacts with Brønsted

acid sites to form strongly hydrogen-bonded species involving bridging OH groups [17]. Turning our attention to the ν(OH) region, the presence of a negative band at 3670 cm^{-1}, after evacuation at 423 K, is in favour of a strong hydrogen bound state.

In contrast, a protonated state is evidenced by using lutidine considered as the most basic probe. In addition to the silanol perturbation, other hydroxyl groups perturbed at 3661 and 3630 cm^{-1} are observed. Those two hydroxyl components are considered to be characteristic of beidellite [12]. The beidellite character is due to a substitution of Si^{4+} by Al^{3+} in tetrahedral coordination with interlayer cations to balance the resulting negative deficiency [12]. It is possible that in the case of acid-treated bentonite, the protons, balancing the negative charge in tetrahedral sites like

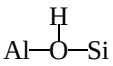

represent a fraction of strongly acidic hydroxyls. This isomorphous substitution of Si^{IV} by Al^{III} in tetrahedral layers [31,32] is responsible for both Lewis and Brønsted acidity [33–35].

The presence of Al both in tetrahedral and octahedral positions in the acid-treated bentonite is demonstrated by using ^{27}Al MAS NMR [9] as in the case of zeolites [36]. The signal at 57.28 ppm is assigned to a fraction of Al in the tetrahedral layers, whereas the signal at 0.412 ppm is due to the octahedrally coordinated Al in the lattice of acid-treated bentonite.

Another tentative identification of aluminum in tetrahedral coordination has been made by using elemental analysis results on the basis of the general formulae of aluminosilicate type: montmorillonite and beidellite described by Mering for one half cell [37]:

$$[Si_{4-x}Al_x]^{IV}[(Al+Fe)_{2-y}Mg_y]^{VI}$$

if $x = 0$ ideal montmorillonite, and if $y = 0$ ideal beidellite.

The exploitation of the data gives rise to the following distribution in tetrahedral and octahedral layers:

Atoms	Si^{IV} Al^{IV}	Al^{IV} Fe^{VI} Mg^{VI}
1/2 cell	$3.89 + 0.11$	$0.86 + 0.05 + 0.09$
Total	4	1

In summary, ^{27}Al MAS NMR shows the presence of Al^{3+} in tetrahedral coordination of the acid-treated bentonite and infrared spectroscopy reveals their acidic role.

5. Conclusion

The propan-2-ol transformation well reflects the acid character of acid-treated bentonite. The catalytic activity shows an overall acidity, whereas the selectivity accounts for the nature of the acid sites. The appearance of ether derived necessarily from propan-2-ol at low temperature accounts for the Brønsted acid sites; these involved acid sites seem to be associated with interlayer cations. The alcohol dehydration into propene seems related to the Lewis acid sites considered to be the most abundant.

The examination of the IR spectra using different basic probes such as: 2,6-dimethylpyridine and CD_3CN shows the presence of various types of acid sites. The Lewis acid sites and the involvement of SiOH groups are well characterised by pyridine and CD_3CN adsorption. In contrast, lutidine adsorption reveals both the existence of Brønsted acid sites and the presence of hydroxyl groups characteristic of beidellite. The potential site created by Al in tetrahedral layers is confirmed by using ^{27}Al MAS NMR.

We can conclude that the residual acidity of acid bentonite is principally constituted by Lewis acid sites present on the surface.

Acknowledgement

The authors thank Dr. J.C. Roussel of the Petroleum French Institute for carrying out the solid-state ^{27}Al MAS NMR characterisation. We also acknowledge the Algerian supplier for providing acid-treated bentonite.

References

[1] C.N. Rhodes and D.R. Brown, J. Chem. Soc. Faraday Trans. I 89 (1995) 1387.
[2] C.N. Rhodes and D.R. Brown, Catal. Lett. 24 (1994) 285.
[3] J.M. Zyla and A. Kryzanowski, Miner. Pol. (1988) 19.
[4] J.A. Ballantine, J.H. Purnell and J.M. Thomas, J. Mol. Catal. 27 (1984) 157.
[5] Y. Guiyang, C. Change, L. Shen, H. Ying, X. Limin and W. Wengo, Chem. Abstr. Phys. Organ. Chem. 22 (1997) 135554.
[6] A. Gervanisi, J. Fenyvesi and A. Auroux, Catal. Lett. 43 (1997) 219.
[7] M.A. Aramendia, V. Boreau, C. Jiménez, J.M. Martina, A. Porras and F.J. Urabano, React. Kinet. Catal. Lett. 53 (1994) 397.
[8] H.D. Morris, S. Bank and P.D. Ellis, J. Phys. Chem. 94 (1990) 3121.
[9] C.N. Rhodes and D.R. Brown, J. Chem. Soc. Faraday Trans. 91 (1995) 1031.
[10] P.T. Hang and G.W. Brindly, Clays Clays Miner. 18 (1970) 203.
[11] M.S. Joshi and P. Moan Rao, J. Colloid. Interface Sci. 95 (1983) 132.
[12] V.C. Farmer and J.D. Russel, Spectrochim. Acta 20 (1964) 1158.
[13] C. Lahousse, F. Maugé, J. Bachelier and J.C. Lavalley, J. Chem. Soc. Faraday Trans. 91 (1995) 2907.
[14] E.M. Frafan-Torrès, E. Sham and P. Grande, Catal. Today 15 (1992) 515.
[15] J.R. Butrille and T.J. Pinnavaia, Catal. Today 14 (1992) 141.
[16] P.O. Sckart, F.D. Declerck, R.E. Sempels and P.G. Rouxhet, J. Chem. Soc. Faraday Trans. I 73 (1977) 359.
[17] A.G. Pelmenskchikov, R.A. van Santen, J. Janchen and E. Meijer, J. Phys. Chem. 97 (1993) 11071.
[18] M.H. Healy, L.F. Wieserman, E.M. Arnett and L.K. Wefers, Langmuir 5 (1989) 114.
[19] M. Ziolek, I. Nowak and J.C. Lavalley, Catal. Lett. 45 (1997) 259.
[20] D. Coster, A.L. Blumenfeld and J.J. Fripiat, J. Phys. Chem. 98 (1994) 6201.
[21] D. Eberel, Clays Clays Miner. 26 (1978) 327.

[22] H. Van Damme, F. Bergaya and L. Gatineau, J. Chim. Phys. 84 (1987) 1075.
[23] C.N. Rhodes and D.R. Brown, Catal. Lett. 45 (1997) 35.
[24] J.M. Serratoza, Clays Clays Miner. 14 (1966) 3858.
[25] R. Mokaya and W. Jones, J. Catal. 153 (1995) 76.
[26] T. Cseri, S. Békassy, F. Figueras and S. Rizner, J. Mol. Catal. A 98 (1995) 101.
[27] A. Janin, M. Maache, J.C. Lavalley, J.F. Joly, F. Raatz and N. Szydlowski, Zeolites 11 (1991) 391.
[28] C.R. Theocharis, K.J. s'Jacob and A.C. Gray, J. Chem. Soc. Faraday Trans. I 84 (1988) 1509.
[29] C.L. Angell and M.V. Howell, J. Phys. Chem. 75 (1969) 2551.
[30] R.I. Soltanov, E.A. Paukshtis and E.N. Yurchenko, React. Kinet. Catal. Lett. 34 (1987) 421.
[31] J.M. Adams, T.V. Clapp, D.E. Clement and P.I. Reid, J. Mol. Catal. 27 (1984) 179.
[32] M.M. Mortland and K.V. Raman, Clays Clays Miner. 16 (1968) 363.
[33] S. Narayanan and K. Despande, J. Mol. Catal. A 104 (1995) 109.
[34] A.K. Galwey, J. Catal. 19 (1970) 330.
[35] J.J. Fripiat, A. Léonard and J.B. Uytterhoeven, J. Phys. Chim. 69 (1965) 10.
[36] P.V. Shertukde, W.K. Hall, J.M. Dereppe and G. Marcelin, J. Catal. 139 (1993).
[37] J. Mering, *Encyclopedia of Soil Sci.* (1975) p. 97.